Incorporating Bacteria as a Living Component in Supramolecular Self-Assembled Monolayers through Dynamic Nanoscale Interactions

Shrikrishnan Sankaran, Mustafa Can Kiren, and Pascal Jonkheijm*

Laboratory group of Bioinspired Molecular Engineering, Molecular Nanofabrication Group, Faculty of Science and Technology and MESA+ Institute for Nanotechnology, University of Twente, P.O. Box 217, Enschede 7500AE, The Netherlands

ABSTRACT Supramolecular assemblies, formed through noncovalent interactions, has become particularly attractive to develop dynamic and responsive architectures to address living systems at the nanoscale. Cucurbit[8]uril (CB[8]), a pumpkin shaped macrocylic host molecule, has been successfully used to construct various self-assembled architectures for biomedical applications since it can simultaneously bind two aromatic guest molecules within its cavity. Such architectures can also be designed to respond to external stimuli. Integrating living organisms as an active component into such supramolecular architectures would add a new dimension to the capabilities of such systems. To achieve this, we have incorporated supramolecular functionality at the bacterial surface by genetically modifying a transmembrane protein to display a CB[8]-binding motif as part of a cystine-stabilized miniprotein. We were able to confirm that this supramolecular motif on the bacterial surface specifically binds CB[8] and forms multiple intercellular ternary complexes leading to aggregation of the bacterial solution. We performed various aggregation experiments to understand how CB[8] interacts with this bacterial strain and also demonstrate that it can be chemically reversed using a competitor. To confirm that this strain can be incorporated with a CB[8] based architecture, we show that the bacterial cells were able to adhere to CB[8] self-assembled monolayers (SAMs) on gold and still retain considerable motility for several hours, indicating that the system can potentially be used to develop supramolecular bacterial biomotors. The bacterial strain also has the potential to be combined with other CB[8] based architectures like nanoparticles, vesicles and hydrogels.

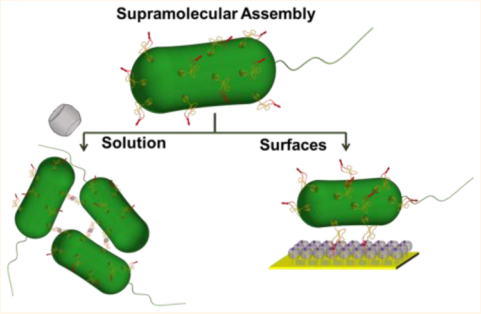

KEYWORDS: supramolecular · Cucurbit[8]uril · *E. coli* · bacterial display · eCPX · knottins · aggregation · self-assembled monolayers

In nature, complex cellular processes are almost entirely mediated through dynamic noncovalent interactions between individual molecules or their assemblies. For example, bacteria communicate with their environment through fascinating processes in which natural supramolecular complexes form and disassemble rapidly, allowing for behaviors like chemotaxis, quorum sensing, surface adhesion and biofilm formation. The understanding of such processes has led to the development of powerful synthetic strategies that enable us to dynamically address living cells at the nanoscale. One approach has involved developing self-assembly based responsive supramolecular materials for bacterial detection,[1−3] antimicrobial therapies[4] and even bacterial biomotor systems.[5,6] An alternative but powerful approach that is still in its infancy involves tailoring supramolecular building blocks directly into the membranes of living cells. For example, Bertozzi and co-workers presented short oligonucleotides on cell surfaces *via* a metabolic labeling approach to allow for further cellular assembly through DNA hybridization.[7] Very recently Kros and co-workers reported a liposome fusion process to introduce cholesterol functionalized coiled-coil forming peptides, which allowed for the *in vivo* decoration of cellular membranes.[8] In prior work by Yousaf and co-workers, such liposome fusion strategies were shown to yield three-dimensional tissue-like structures.[9] These studies not only show us that innovative approaches are required to address cells at the molecular level but also stress that we need to clearly understand the nature of the interactions

* Address correspondence to p.jonkheijm@utwente.nl.

Received for review January 30, 2015 and accepted March 4, 2015.

Published online March 04, 2015
10.1021/acsnano.5b00694

between our synthetic molecules and complex cellular environments.

To perform such studies, supramolecular architectures with mechanical, optical and electrochemical functionalities have been developed through careful design of molecular building blocks.[10−13] Since these architectures utilize dynamic noncovalent interactions similar to those seen in biological systems, it has become particularly attractive to adopt them for mimicking cellular functions.[14] For such purposes host−guest systems involving macrocyclic host molecules and aromatic guests have gained a lot of attention since their binding properties are similar to those of proteins. One such group of host molecules, which have been shown to be extremely successful in developing constructs and platforms for biosensing and manipulating living cells, are Cucurbit[*n*]urils (CB[*n*]). These are macrocyclic host molecules composed of methylene-linked glycoluril monomers. They are symmetric and "barrel"-like in shape with two identical portal regions laced by ureido-carbonyl oxygens.[15,16] Recently, the microscopic recognition properties of CB[n] have been exploited to create protein nanowires,[17] chemical sensors,[18] molecular machines,[19] supramolecular materials,[20] protein chips[21] and drug delivery systems.[22−24] In particular, the selective binding of specific amino acid side chains to CB[*n*] has been exploited for sensing of protonated and aromatic residues.[25−28] In contrast to the smaller CB[*n*] homologues, CB[8] has a larger cavity volume capable of simultaneously accommodating two aromatic amino acids, such as phenylalanine and tryptophan in a $\pi-\pi$ stack geometry to form 2:1 homoternary complexes.[29] This binding motif has found application in the dimeric and tetrameric assembly of proteins[30−32] and in hydrogel formation.[33] On the other hand, multiresponsive bioactive molecular platforms have been developed by using heteroternary complexes involving functional molecules conjugated to, *e.g.*, methylviologen, naphthol, or azo-benzene.[34,35] These systems have been used to target proteins and living cells in a manner that can be reversed by applying photochemical and electrochemical stimuli. As the next step, we envisioned that a new dimension of functionality can be introduced to such supramolecular architectures by incorporating living bacterial cells as an active component. This would open up possibilities to endow interesting properties to these dynamic supramolecular architectures like motility, self-repair, incorporation of engineered proteins, *etc.*

To achieve this, we have developed a novel strategy to introduce specific, dynamic and reversible supramolecular functionality on the bacterial cell surface by adopting a bacterial display system that has been used before exclusively to identify high affinity peptides for various proteins. This technique involves fusing a cystine-stabilized miniprotein bearing randomized peptide sequences to the N-terminus of a modified transmembrane protein (enhanced Circularly Permutated outer membrane protein X, eCPX).[36,37] Using this powerful technique to render chemical functionality to the bacterial surface has not yet been explored. Accordingly, we show that a bacterial strain with supramolecular functionality can be developed by displaying a miniprotein that can reversibly bind with the supramolecular host molecule cucurbit[8]uril (CB[8]). Peptides containing tryptophan or phenylalanine like FGG, WGG, GGFGG, and GGWGG have been shown to bind CB[8] with dissociation constants in the low micromolar (μM) range.[38,39] For our supramolecularly addressable bacterial strain, we grafted the GGWGG sequence into one loop of a cystine stabilized miniprotein named Min-23 (**1**), then genetically fused this to the N-terminal of eCPX and expressed it in an MC1061 strain of *Escherichia coli*(Chart 1). Since bacterial expression systems produce multiple copies of the cloned protein, we postulated that multivalent interactions could be established between bacterial cells in the presence of CB[8], resulting in their aggregation. Few reports exist on the use of multivalent host−guest interactions for macroscopic self-assembly, *e.g.*, the assembly of cyclodextrin-functionalized and guest-functionalized hydrogels and adhesion of CB-functionalized silicon chips with guest-functionalized counterparts.[40,41] However, in living systems like bacteria, various voluminous cell surface components like flagellae and pili could prevent CB[8] from accessing miniproteins on two separate bacterial cell membranes. Also, CB[8] could probably bind only adjacent miniprotein guests on the same bacterial surface, preventing aggregation and self-assembly onto monolayers. Finally, unspecific interactions between CB[8] and aromatic amino acids on other transmembrane proteins could possibly reduce the specificity of the system. Despite these potential hurdles, we were able to clearly show that specific intercellular supramolecular interactions are established by ternary complex formation between CB[8] and two miniprotein guests, causing bacterial assembly in solution and surfaces. We used this phenomenon to study the characteristics of the interactions between CB[8] and our bacterial strain. Once we gained a clear understanding of the interaction, we tested the assembly of this bacterial surface on CB[8] modified self-assembled monolayers (SAMs). We attained specific and reversible adhesion of our bacterial cells on these surfaces and saw that the cells even retained their motility indicating that the noncovalent interactions allow the cells to remain active.

RESULTS AND DISCUSSION

Display of Miniproteins. First we wanted to test whether our modified miniproteins were displayed on the surface of our bacterial cells. As negative control in all experiments, a β-trypsin inhibitor knottin (**2**)[42] was

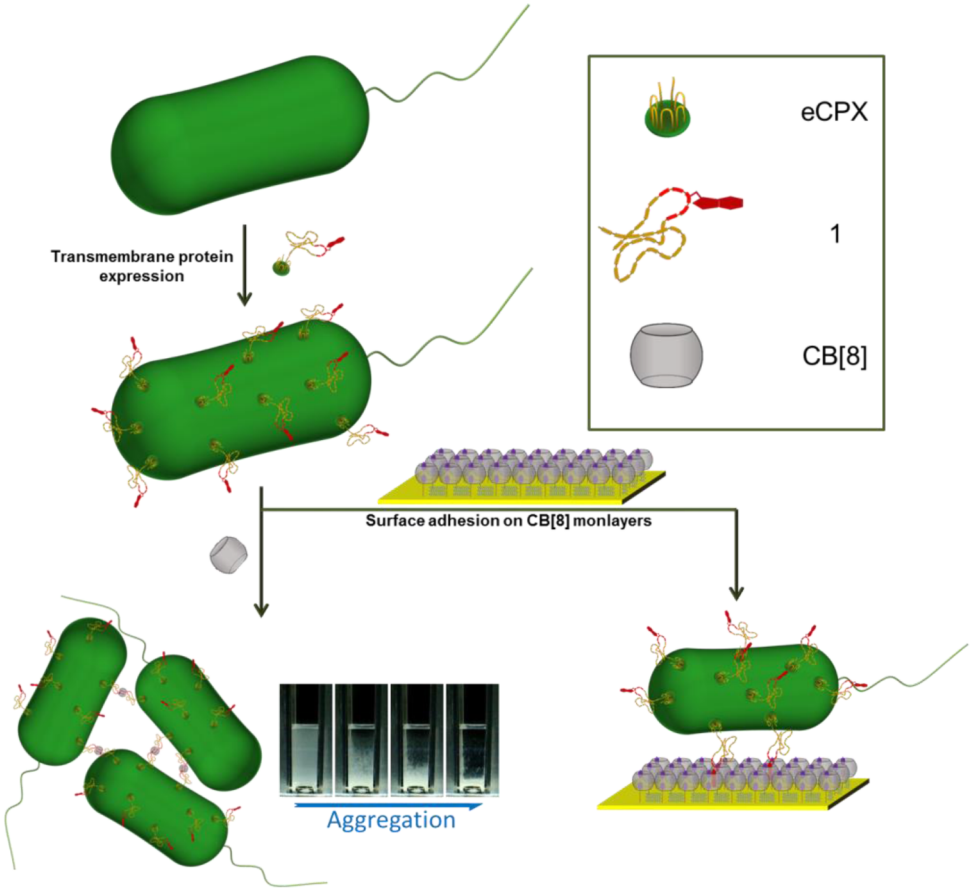

Chart 1. Development of a CB[8]-addressable bacterial strain. Min-23 construct 1 contains peptide sequence GGWGG in one loop. This was genetically fused to a modified outer membrane protein eCPX, which enabled it to be displayed on the outer membrane and bind CB[8].

separately expressed and fused to the N-terminal of eCPX. We attempted a quick detection of these two membrane proteins using SDS-PAGE from cell lysates despite their low expression yields and poor solubility. However, a modified strategy of expressing the proteins overnight and increasing solubility of the lysis buffer by including a detergent and a denaturing agent was employed. This enabled us to observe bands of expected molecular weights corresponding to the miniproteins conjugated to eCPX (Supporting Information Figure S1). Flow cytometry experiments with fluorescein isothiocyanate (FITC)-labeled trypsin were carried out as an additional verification that the miniproteins were being displayed (Supporting Information Figure S2). We could clearly see that the strain displaying the β-trypsin inhibitor knottin had a large population that was fluorescently labeled.[43] In a prior work, the number of displayed peptides has been estimated to be in the order 10^3-10^4 on the bacterial surface.[43]

Supramolecular Assembly of Bacteria in Solution. In the case of the strain engineered to display our GGWGG peptide sequence-containing miniprotein **1**, we expected that CB[8] could cause aggregation of a bacterial culture if the miniproteins were sufficiently accessible. To test whether such supramolecular assembly would occur despite the hurdles mentioned before, we prepared solutions containing 25 μM CB[8] and the bacteria displaying **1** and **2**. Within 20 min, aggregation was visible to the naked eye in culture displaying **1** and was recorded as shown in Figure 1 (Supporting Information Video S1). In the next 10 min, nearly all the bacteria had been pulled down. In the culture displaying **2**, some aggregation was seen around 50 min but appeared gradual and led to less than a third of the culture being pulled down over a total time of 90 min. These results were also recorded by measuring the optical density of the cultures at 600 nm (Supporting Information Figure S3). To enlarge the probing volume and simultaneously record multiple samples, we opted to quantify the data from the recorded videos by taking the mean gray value of the cultures as a measure of the bacterial density while monitoring at constant light intensity (Figure 1b and Supporting Information Video S1). The specificity of the assembly was always verified using the bacterial culture displaying **2** as a negative control while performing all the ensuing experiments. Staining the cells with Hoechst dye 33342 enabled us to clearly see that over large areas the bacterial cells displaying **2** are

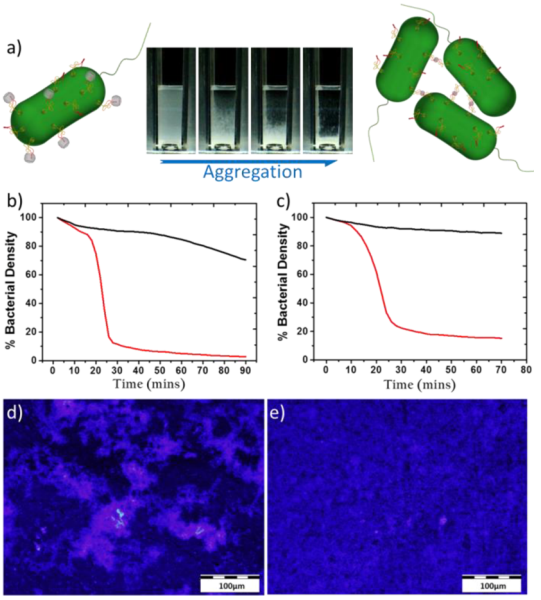

Figure 1. (a) Snapshot images of the aggregation of bacteria in solution upon addition of CB[8]. Plots displaying aggregation kinetics using (b) 1.0 $OD_{600\,nm}$ bacterial solutions displaying 1 (red) and 2 (black) with 25 μM CB[8], (c) 1.0 $OD_{600\,nm}$ bacterial solutions displaying 1 with 25 μM CB[8] (red) and CB[7] (black). Epifluorescence microscopy images of H33342 stained bacteria forming clusters when mixed with CB[8] in the case of cells displaying 1 (d) and absence of clusters seen in the case of cells displaying 2 (e).

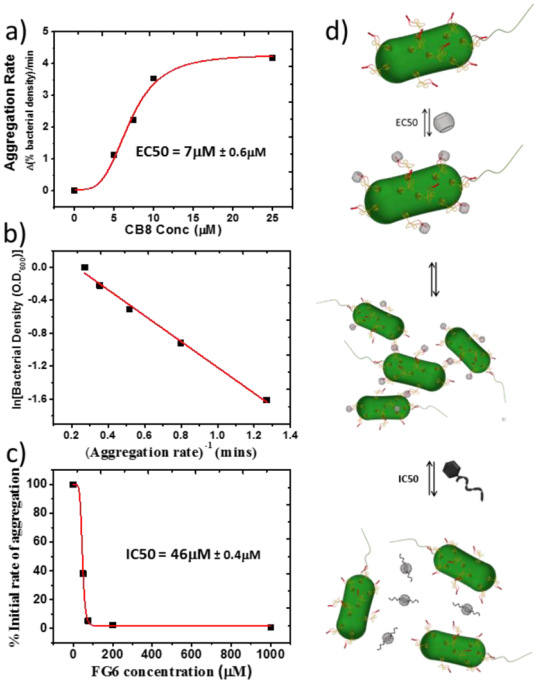

Figure 2. (a) Aggregation rates *vs* CB[8] concentration fitted with Supporting Information eq S1 to obtain an EC_{50} value. (b) ln(Bacterial density) *vs* reciprocal of aggregation rate with a linear fit indicating first-order kinetics. (c) Reduction in the rate of aggregation plotted as a % of initial aggregation against different concentrations of FG6 fitted to Supporting Information eq S1. (d) Proposed mechanism of aggregation and reversibility with each step of the process next to the plots analyzing the corresponding kinetics.

distributed quite homogeneously (Figure 1d), while those displaying **1** are aggregated into clusters (Figure 1e). To further verify that aggregation is caused specifically by ternary complex formation, we used CB[7] as a negative control as the smaller cavity size of CB[7] can host only one tryptophan at a time. As expected, aggregation rapidly occurred only in the culture mixed with 25 μM CB[8], while no aggregation was witnessed in the culture mixed with 25 μM CB[7] even after a much longer time (Figure 1c and Supporting Information Video S2).

Confident that the assembly occurred due to specific intercellular interactions between CB[8] and our surface-displayed miniproteins, we decided to study some characteristics of this supramolecular phenomenon. Accordingly, we performed aggregation experiments with different CB[8] concentrations and found that the rate was clearly dependent on this parameter (Supporting Information Figure S4 and Video S3). Plotting the aggregation rates against CB[8] concentrations gave us a binding-curve (Figure 2a) from which we derived (using Supporting Information eq S1) an EC_{50} value of around 7 μM. As expected, this is within an agreeable range for the binding of CB[8] with such aromatic amino acid containing peptides. Depending on the peptide sequence and the N/C terminal nature of the aromatic amino acid, it has been determined that CB[8] binds with dissociation constants ranging from 10^{-6} to 10^{-3} M as shown in the Supporting Information (Table S1). Subsequently, we also performed aggregation experiments keeping CB[8] concentration at 25 μM and varying the bacterial densities. The rate of aggregation increased with higher bacterial densities as seen in Supporting Information Figure S5 and Video S4. To determine the order of the aggregation event, we took bacterial density as concentration and the reciprocal of aggregation rate as time. A plot of ln(Bacterial density) against reciprocal of aggregation rate resulted in a linear trend, appropriately indicating that the complex phenomenon of aggregation follows first order kinetics as a function of bacterial density (Figure 2b). This is most likely due to the fact that the concentration of the surface-displayed miniproteins amounts to low nanomolar (nM) values at the bacterial densities we use. Thus, there is a huge excess of CB[8] available in solution and its concentration does not vary significantly even when all miniproteins are bound to CB[8] molecules. This amount of CB[8] is required to satisfy the affinity requirements for ternary complex formation as determined in Figure 2a but also causes the phenomenon to follow first order kinetics with dependence on bacterial density.

From these experiments, we were able to postulate a simplified mechanism for the aggregation (Figure 2d), similar to some that have been proposed to explain aggregation of lipid vesicles.[44] In this model, we propose that a first quick step occurs where the CB[8] binds

to the GGWGG motif on the bacterial surface since CB[8] concentration is several orders higher than the GGWGG motif (low nM range). Thus, the coverage of CB[8] on the bacterial surface varies with CB[8] concentration. This converts the bacterial cells into active binding entities that are able to stick to each other on collision. First, clusters form and grow in size leading to aggregation. Since this step depends on the number of collisions that occur over time, varying the bacterial density has a direct influence on the rate of aggregation.

The ability to reverse the effects of supramolecular interactions is a powerful property of such systems. Agitation of an aggregated sample disperses the bacteria in solution as smaller clusters but aggregation reoccurs when the agitation is stopped. To reverse the aggregation effect, we selected a peptide with an N-terminal phenylalanine followed by 6 glycines (FG6) as a CB[8] competitor. We first performed cell viability tests, which ensured that FG6 was not cytotoxic (Supporting Information Figure S6). To study the inhibition of aggregation, we initially allowed bacterial solutions to aggregate in the presence of 25 μM CB[8]. Different concentrations of FG6 up to 1 mM were then added to each sample and the mixtures were briefly agitated by mild shaking. The agitation was then stopped and reaggregation was monitored. The sample with no added FG6 aggregated rapidly, whereas those in which FG6 was added aggregated at rates depending on the FG6 concentration (Supporting Information Figure S7 and Video S5). The degree to which the rate of aggregation reduced in the presence of FG6 was taken as a measure of the extent of inhibition. This, calculated as percentage, when plotted against FG6 concentration, provided a trend, from which we were able to derive an inhibition constant (IC_{50}) of 46 μM using Supporting Information eq S1 (Figure 2c), indicating that the addition of a soluble competitive guest peptide inhibits the association of bacteria by blocking all of the available CB[8] hosts.

Motile Surface-Bound CB[8] Addressable Bacteria. Having confirmed the supramolecular nature of the interaction between the bacterial surface and CB[8] and determined its various characteristics, we intended to show that the bacterial strain could be incorporated into an existing molecular architecture of CB[8]. We had previously shown that it was possible to use self-assembled monolayers (SAMs) of CB[8], noncovalently displaying an RGD motif, for reversible cell adhesion.[45] Incorporating our bacterial strain into these SAMs would allow the possibility to introduce interesting properties to the architecture. It has been shown previously that, by adhering bacterial cells to surfaces, their motility can be used to convert chemical energy into mechanical energy for micron scale devices.[5,6] We thought our bacterial cells on CB[8]-bearing surfaces would still retain a certain extent of motility due to the noncovalent nature of the adhesion. Also, in this system, we avoid chemical modification of the bacterial surface, which is usually prone to alter properties of cells.

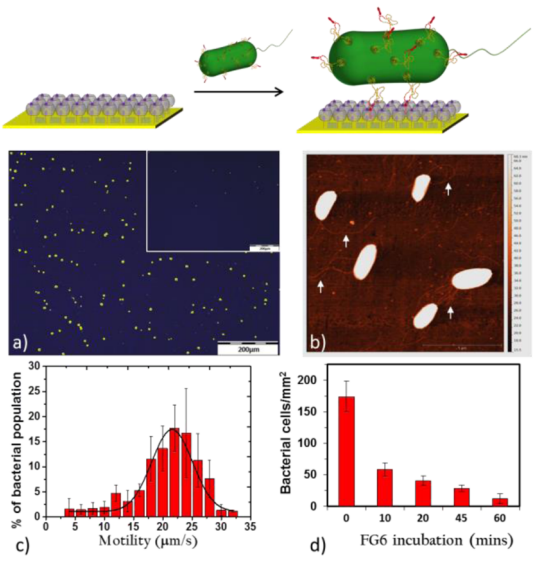

Figure 3. Bacterial surface immobilization. (a) Bacterial cells displaying 1 immobilized in significant numbers compared to bacterial cells displaying 2 (inset). Bacterial cells have been provided false colors to improve their visibility. (b) *E. coli* cells and their flagellae (indicated by the arrows) seen using high resolution AFM. (c) Distribution of the motility of immobilized bacteria fitted with the Gaussian function. Average rate of motility and deviation values were determined from 4 individual videos spanning 50 s with approximately 30 motile bacterial cells in each. (d) Bacterial cells/mm^2 remaining on the surface *vs* amount of time the surface was incubated with FG6. Bacterial counts and deviations were obtained from 4 separate representative images.

To test this out, we first attempted to immobilize our bacteria onto CB[8] monolayers. The monolayers were prepared on gold using a strategy to insert CB[8]-methylviologen thiol inclusion complexes into a repellent monolayer as described previously by us.[40] On incubation of such substrates with bacteria displaying **1** and **2**, we observed that the bacterial cells displaying **1** adhered in much greater numbers than the cells displaying **2** (Figure 3a). Using atomic force microscopy (AFM), we were able to obtain higher resolution images of the immobilized bacterial cells with their flagellae seen as thin twisted fibers (Figure 3b).

With the use of a flow cell, we allowed bacterial cells displaying **1** to adhere to CB[8] monolayers and flushed with buffer to remove nonspecifically adhered bacteria. The specifically surface bound bacteria were highly motile, tracing long paths with considerable speed (Supporting Information Video S6). Surprisingly, the rate of motility that we observed was much higher than that of other techniques found in literature.[5] This movement at the surface was seen for up to 4 h without alteration even when the flow cell was turned upside down or a flow of 1 mL/min was employed. The rate of motility seems to follow a Gaussian distribution with a peak close to 20 μm/s (Figure 3c). In comparison,

motile *E. coli* cells in solution are known to reach speeds of 20−40 μm/s indicating that supramolecular surface immobilization barely hinders this motility. To test the reversibility of this binding, we used the CB[8]-binding peptide FG6. As expected, most of the bacteria rapidly detached from the surface. Figure 3d indicates that within the first 10 min a majority of the cells detach and at 60 min very few isolated cells are still seen at the surface. The detachment follows first order kinetics with an observed first-order dissociation rate constant of about 0.13 min^{-1}.

CONCLUSION

In conclusion, we have successfully developed a supramolecularly accessible bacterial strain that can be used in conjunction with supramolecular architectures in solution and surfaces. The current study focuses on specificity toward CB[8], but the techniques presented can also be used to develop and study other strains for different host molecules. It would even be possible to recombinantly transfer this modified transmembrane protein to other bacterial strains like *Shigella* and *Salmonella*, which also express the outer membrane protein X. Currently, we are modulating the characteristics of the surface based interactions and looking into applying this bacterial strain with other supramolecular architectures. Furthermore, we demonstrate that the bacterial cells were able to adhere to CB[8] monolayers and still retain considerable motility for several hours indicating that the system can be used to develop supramolecular bacterial biomotors, which hold the promise to become a macroscopic alternative to molecular motors.[46]

METHODS

Cloning of E. coli Expression Plasmids. Plasmid pB33eCPX was a gift from Patrick Daugherty (Addgene plasmid # 23336). It contained the gene of the enhanced circularly permutated outer membrane protein X (eCPX). The DNA sequences of **1** and **2** were purchased from Eurofins MWG Operon. These sequences were ligated between OmpX signal sequence and eCPX using BsrGI and NheI restriction sites, which were introduced as follows. OmpX was amplified with a BsrGI site at its 3′end and eCPX was amplified with a NheI site at its 5′-end. **1** and **2** were amplified with BsrGI and NheI restriction sites at their 5′- and 3′-ends. These three amplified constructs and the plasmid were digested with appropriate restriction enzymes, purchased from NEB, and ligated together in one reaction. These ligated products were transformed into NovaBlue competent cells (Novagen) and plated on LB-Chloramphenicol agar plates. Plasmids extracted from colonies were sequenced, and ones with the correct sequences were transformed into MC1061 competent cells from Invitrogen. The final constructs were of the form (OmpX Signal sequence−Thrombin cleavage site−Cystine stabilized miniprotein−eCPX). Miniprotein primary sequences **1**−GGWGG in Min-23 scaffold, LMRCKQDSDCLAGSVCGGWGGFCG; and **2**−β-Trypsin inhibitor knottin, RVCPRILMECKKDSDCLAECVCLEHGYCG.

Bacterial Experiments. Five milliliters of LB and 34 μg/mL chloramphenicol (Cam) medium was inoculated with glycerol stock bacteria displaying **1** and **2** and incubated overnight at 37 °C with 250 rpm shaking. Next, 100 μL of these cultures was then added into fresh 5 mL of LB−Cam media and allowed to grow for 2 h at 37 °C and 250 rpm. This was then induced with 0.04% (w/v) L-arabinose and incubated at 37 °C with 250 rpm for 2 h. For fluorescent microscopy related experiments, 1 μg/mL Hoechst 33342 dye was added and allowed to stain the cells for 10 min. The cultures were then spun down at 6000*g* for 10 min. The supernatant was discarded, 5 mL of HEPES (10 mM) NaCl (137 mM) buffer was added, and the cells were resuspended. This was repeated twice to wash the cells. Finally, HEPES NaCl buffer was added in appropriate quantities to provide a solution with desired bacterial density. Bacterial cell density was determined using a Biochrom WPA CO8000 Cell Density meter. An Olympus microscope IX71 with filters was used for recording fluorescent images. AFM images were recorded using an NTegra Spectra from NT-MDT. Real time images of bacterial aggregation were taken using a Veho VMS-004 deluxe microscopic camera. Image processing and analysis was done using ImageJ. The data was plotted using Microcal Origin 8.0.

Cucurbituril Solutions. Cucurbit[8]uril and cucurbit[7]uril were purchased from Sigma-Aldrich. Due to poor solubility of CB[8] in water and its hygroscopic nature, the apparent molecular weight of the commercial powder and its actual concentration in aqueous solutions were determined for each batch using a simple and highly reproducible method described previously.[47]

FG6 Peptide. The FG6 peptide was a gift from Emanuela Cavatorta, produced by solid phase peptide synthesis and purified using reverse phase HPLC.

Preparation of SAMs on Gold. Gold substrates were first washed with piranha solution (H_2SO_4 and 30% H_2O_2, v/v 70/30), and copious amounts of milli-Q water afterward. Substrates were then immersed into a mixed solution of 0.1 mM triethylene glycol and 2-mercaptoethanol at a ratio of 99:1 (v/v) for 3 min, washed with water, and dried with N_2. The binary complex of methyl viologen thiol/CB[8] was formed at the concentration of 50 μM, and was back-inserted into triethylene glycol modified gold surfaces by overnight incubation. After the complex was rinsed with water for 5 min, the substrates were used for bacterial immobilization experiments.

Bacterial Immobilization Experiments. The CB[8] monolayers on gold were incubated with H33342 stained 0.01 $OD_{600\ nm}$ bacterial solutions containing 50 μM CB[8] for 1 h. The substrates were then washed thoroughly with water and dried. These cells were then visualized using and epifluorescence microscope.

Bacterial Surface Motility Experiments. We used a macroscopic flow cell having CB[8] monolayers on a 20 nm thick 1 in. circular gold substrate on one side and a glass window on the other, enabling us to obtain images from either side. A solution containing 50 μM CB[8] and 0.01 $OD_{600\ nm}$ bacteria displaying **1** was flowed into the chamber and the bacteria were allowed to bind without flow for 30 min. This was followed by flushing the chamber with buffer and capturing images and videos of the motile cells in bright field mode. A 0.5 mM FG6 solution was flowed into the chamber and incubated for 1 h during which almost all the cells released. Supporting Information Video S7 was taken after 10 min of FG6 incubation when few cells were still seen attached.

Conflict of Interest: The authors declare no competing financial interest.

Supporting Information Available: Experimental procedures, additional characterization data, analysis details and videos. This material is available free of charge *via* the Internet at http://pubs.acs.org.

Acknowledgment. We thank Shyam Sankaran for his contribution towards the image processing, Jasper van Weerd for his help in recording the AFM images and Emanuela Cavatorta for providing the FG6 peptide. We also thank Dr. Jennifer Getz

and Prof. Patrick Daugherty from the University of California, Santa Barbara, for providing a very clear procedure on how to establish a bacterial display system and their prompt and helpful replies to several questions regarding the same. S.S. developed the bacterial strains and performed all the aggregation and surface immobilization experiments. M.C.K. was involved in setting up the bacterial display system and analyzing it by FACS and SDS-PAGE. P.J. supervised the entire project and, along with S.S., designed the experiments, analyzed the data and drafted the manuscript. This research was funded by St-ERC grant Sumoman (259183).

REFERENCES AND NOTES

1. Ryu, J.-H.; Lee, E.; Lim, Y.; Lee, M. Carbohydrate-Coated Supramolecular Structures: Transformation of Nanofibers into Spherical Micelles Triggered by Guest Encapsulation. *J. Am. Chem. Soc.* **2007**, *129*, 4808–4814.
2. Müller, M. K.; Brunsveld, L. A Supramolecular Polymer as a Self-Assembling Polyvalent Scaffold. *Angew. Chem., Int. Ed.* **2009**, *48*, 2921–2924.
3. Yu, G.; Ma, Y.; Han, C.; Yao, Y.; Tang, G.; Mao, Z.; Gao, C.; Huang, F. A Sugar-Functionalized Amphiphilic Pillar[5]arene: Synthesis, Self-Assembly in Water, and Application in Bacterial Cell Agglutination. *J. Am. Chem. Soc.* **2013**, *135*, 10310–10313.
4. Lui, L. T.; Xue, X.; Sui, C.; Brown, A.; Pritchard, D. I.; Halliday, N.; Winzer, K.; Howdle, S. M.; Fernandez-Trillo, F.; Krasnogor, N. Bacteria Clustering by Polymers Induces the Expression of Quorum-Sensing-Controlled Phenotypes. *Nat. Chem.* **2013**, *5*, 1058–1065.
5. Rozhok, S.; Shen, C. K.-F.; Littler, P.-L. H.; Fan, Z.; Liu, C.; Mirkin, C. A.; Holz, R. C. Methods for Fabricating Microarrays of Motile Bacteria. *Small* **2005**, *1*, 445–451.
6. Hiratsuka, Y.; Miyata, M.; Tada, T.; Uyeda, T. Q. P. A Microrotary Motor Powered by Bacteria. *Proc. Natl. Acad. Sci. U.S.A.* **2006**, *103*, 13618–13623.
7. Gartner, Z. J.; Bertozzi, C. R. Programmed Assembly of 3-Dimensional Microtissues with Defined Cellular Connectivity. *Proc. Natl. Acad. Sci. U.S.A.* **2009**, *106*, 4606–4610.
8. Zope, H. R.; Versluis, F.; Ordas, A.; Voskuhl, J.; Spaink, H. P.; Kros, A. *In Vitro* and *in Vivo* Supramolecular Modification of Biomembranes Using a Lipidated Coiled-Coil Motif. *Angew. Chem., Int. Ed.* **2013**, *52*, 14247–14251.
9. Dutta, D.; Pulsipher, A.; Luo, W.; Yousaf, M. N. Synthetic Chemoselective Rewiring of Cell Surfaces: Generation of Three-Dimensional Tissue Structures. *J. Am. Chem. Soc.* **2011**, *133*, 8704–8713.
10. Aida, T.; Meijer, E. W.; Stupp, S. I. Functional Supramolecular Polymers. *Science* **2012**, *335*, 813–817.
11. Fenske, T.; Korth, H.-G.; Mohr, A.; Schmuck, C. Advances in Switchable Supramolecular Nanoassemblies. *Chem.—Eur. J.* **2012**, *18*, 738–755.
12. Yang, L.; Gomez-Casado, A.; Young, J. F.; Nguyen, H. D.; Cabanas-Danés, J.; Huskens, J.; Brunsveld, L.; Jonkheijm, P. Reversible and Oriented Immobilization of Ferrocene-Modified Proteins. *J. Am. Chem. Soc.* **2012**, *134*, 19199–19206.
13. Uhlenheuer, D. A.; Petkau, K.; Brunsveld, L. Combining Supramolecular Chemistry with Biology. *Chem. Soc. Rev.* **2010**, *39*, 2817–2826.
14. Brinkmann, J.; Cavatorta, E.; Sankaran, S.; Schmidt, B.; van Weerd, J.; Jonkheijm, P. About Supramolecular Systems for Dynamically Probing Cells. *Chem. Soc. Rev.* **2014**, *43*, 4449–4469.
15. Lagona, J.; Mukhopadhyay, P.; Chakrabarti, S.; Isaacs, L. The Cucurbit[n]uril Family. *Angew. Chem., Int. Ed.* **2005**, *44*, 4844–4870.
16. Masson, E.; Ling, X.; Joseph, R.; Kyeremeh-Mensah, L.; Lu, X. Cucurbituril Chemistry: A Tale of Supramolecular Success. *RSC Adv.* **2012**, *2*, 1213–1247.
17. Hou, C.; Li, J.; Zhao, L.; Zhang, W.; Luo, Q.; Dong, Z.; Xu, J.; Liu, J. Construction of Protein Nanowires through Cucurbit[8]uril-Based Highly Specific Host–Guest Interactions: An Approach to the Assembly of Functional Proteins. *Angew. Chem., Int. Ed.* **2013**, *52*, 5590–5593.
18. Hennig, A.; Bakirci, H.; Nau, W. M. Label-Free Continuous Enzyme Assays with Macrocycle-Fluorescent Dye Complexes. *Nat. Methods* **2007**, *4*, 629–632.
19. Ko, Y. H.; Kim, E.; Hwang, I.; Kim, K. Supramolecular Assemblies Built with Host-Stabilized Charge-Transfer Interactions. *Chem. Commun.* **2007**, 1305–1315.
20. Appel, E. A.; Barrio, J. del; Loh, X. J.; Scherman, O. A. Supramolecular Polymeric Hydrogels. *Chem. Soc. Rev.* **2012**, *41*, 6195–6214.
21. González-Campo, A.; Brasch, M.; Uhlenheuer, D. A.; Gómez-Casado, A.; Yang, L.; Brunsveld, L.; Huskens, J.; Jonkheijm, P. Supramolecularly Oriented Immobilization of Proteins Using Cucurbit[8]uril. *Langmuir* **2012**, *28*, 16364–16371.
22. Appel, E. A.; Rowland, M. J.; Loh, X. J.; Heywood, R. M.; Watts, C.; Scherman, O. A. Enhanced Stability and Activity of Temozolomide in Primary Glioblastoma Multiforme Cells with Cucurbit[n]uril. *Chem. Commun.* **2012**, *48*, 9843–9845.
23. Kim, E.; Kim, D.; Jung, H.; Lee, J.; Paul, S.; Selvapalam, N.; Yang, Y.; Lim, N.; Park, C. G.; Kim, K. Facile, Template-Free Synthesis of Stimuli-Responsive Polymer Nanocapsules for Targeted Drug Delivery. *Angew. Chem., Int. Ed.* **2010**, *49*, 4405–4408.
24. Ma, D.; Hettiarachchi, G.; Nguyen, D.; Zhang, B.; Wittenberg, J. B.; Zavalij, P. Y.; Briken, V.; Isaacs, L. Acyclic Cucurbit[n]uril Molecular Containers Enhance the Solubility and Bioactivity of Poorly Soluble Pharmaceuticals. *Nat. Chem.* **2012**, *4*, 503–510.
25. Heo, S. W.; Choi, T. S.; Park, K. M.; Ko, Y. H.; Kim, S. B.; Kim, K.; Kim, H. I. Host–Guest Chemistry in the Gas Phase: Selected Fragmentations of CB[6]–Peptide Complexes at Lysine Residues and Its Utility to Probe the Structures of Small Proteins. *Anal. Chem.* **2011**, *83*, 7916–7923.
26. Ghale, G.; Ramalingam, V.; Urbach, A. R.; Nau, W. M. Determining Protease Substrate Selectivity and Inhibition by Label-Free Supramolecular Tandem Enzyme Assays. *J. Am. Chem. Soc.* **2011**, *133*, 7528–7535.
27. Chinai, J. M.; Taylor, A. B.; Ryno, L. M.; Hargreaves, N. D.; Morris, C. A.; Hart, P. J.; Urbach, A. R. Molecular Recognition of Insulin by a Synthetic Receptor. *J. Am. Chem. Soc.* **2011**, *133*, 8810–8813.
28. Logsdon, L. A.; Urbach, A. R. Sequence-Specific Inhibition of a Nonspecific Protease. *J. Am. Chem. Soc.* **2013**, *135*, 11414–11416.
29. Heitmann, L. M.; Taylor, A. B.; Hart, P. J.; Urbach, A. R. Sequence-Specific Recognition and Cooperative Dimerization of N-Terminal Aromatic Peptides in Aqueous Solution by a Synthetic Host. *J. Am. Chem. Soc.* **2006**, *128*, 12574–12581.
30. Dang, D. T.; Nguyen, H. D.; Merkx, M.; Brunsveld, L. Supramolecular Control of Enzyme Activity through Cucurbit[8]uril-Mediated Dimerization. *Angew. Chem., Int. Ed.* **2013**, *52*, 2915–2919.
31. Dang, D. T.; Schill, J.; Brunsveld, L. Cucurbit[8]uril-Mediated Protein Homotetramerization. *Chem. Sci.* **2012**, *3*, 2679–2684.
32. Nguyen, H. D.; Dang, D. T.; van Dongen, J. L. J.; Brunsveld, L. Protein Dimerization Induced by Supramolecular Interactions with Cucurbit[8]uril. *Angew. Chem., Int. Ed.* **2010**, *49*, 895–898.
33. Rowland, M. J.; Appel, E. A.; Coulston, R. J.; Scherman, O. A. Dynamically Crosslinked Materials *via* Recognition of Amino Acids by Cucurbit[8]uril. *J. Mater. Chem. B* **2013**, *1*, 2904–2910.
34. Uhlenheuer, D. A.; Young, J. F.; Nguyen, H. D.; Scheepstra, M.; Brunsveld, L. Cucurbit[8]uril Induced Heterodimerization of Methylviologen and Naphthalene Functionalized Proteins. *Chem. Commun.* **2011**, *47*, 6798–6800.
35. Tian, F.; Jiao, D.; Biedermann, F.; Scherman, O. A. Orthogonal Switching of a Single Supramolecular Complex. *Nat. Commun.* **2012**, *3*, 1207.
36. Rice, J. J.; Daugherty, P. S. Directed Evolution of a Biterminal Bacterial Display Scaffold Enhances the Display of Diverse Peptides. *Protein Eng., Des. Sel.* **2008**, *21*, 435–442.

37. Getz, J. A.; Rice, J. J.; Daugherty, P. S. Protease-Resistant Peptide Ligands from a Knottin Scaffold Library. *ACS Chem. Biol.* **2011**, *6*, 837–844.
38. Bush, M. E.; Bouley, N. D.; Urbach, A. R. Charge-Mediated Recognition of N-Terminal Tryptophan in Aqueous Solution by a Synthetic Host. *J. Am. Chem. Soc.* **2005**, *127*, 14511–14517.
39. Sonzini, S.; Ryan, S. T. J.; Scherman, O. A. Supramolecular Dimerisation of Middle-Chain Phe Pentapeptides *via* CB[8] Host–Guest Homoternary Complex Formation. *Chem. Commun.* **2013**, *49*, 8779–8781.
40. Harada, A.; Kobayashi, R.; Takashima, Y.; Hashidzume, A.; Yamaguchi, H. Macroscopic Self-Assembly through Molecular Recognition. *Nat. Chem.* **2011**, *3*, 34–37.
41. Ahn, Y.; Jang, Y.; Selvapalam, N.; Yun, G.; Kim, K. Supramolecular Velcro for Reversible Underwater Adhesion. *Angew. Chem., Int. Ed.* **2013**, *52*, 3140–3144.
42. Bode, W.; Greyling, H. J.; Huber, R.; Otlewski, J.; Wilusz, T. The Refined 2.0 A X-Ray Crystal Structure of the Complex Formed between Bovine Beta-Trypsin and CMTI-I, a Trypsin Inhibitor from Squash Seeds (Cucurbita Maxima). Topological Similarity of the Squash Seed Inhibitors with the Carboxypeptidase A Inhibitor from Potatoes. *FEBS Lett.* **1989**, *242*, 285–292.
43. Jabaiah, A. M.; Getz, J. A.; Witkowski, W. A.; Hardy, J. A.; Daugherty, P. S. Identification of Protease Exosite-Interacting Peptides That Enhance Substrate Cleavage Kinetics. *Biol. Chem.* **2012**, *393*, 933–941, DOI: 10.1515/hsz-2012-0162.
44. Thomas, G. B.; Rader, L. H.; Park, J.; Abezgauz, L.; Danino, D.; DeShong, P.; English, D. S. Carbohydrate Modified Catanionic Vesicles: Probing Multivalent Binding at the Bilayer Interface. *J. Am. Chem. Soc.* **2009**, *131*, 5471–5477.
45. An, Q.; Brinkmann, J.; Huskens, J.; Krabbenborg, S.; de Boer, J.; Jonkheijm, P. A Supramolecular System for the Electrochemically Controlled Release of Cells. *Angew. Chem., Int. Ed.* **2012**, *51*, 12233–12237.
46. Kudernac, T.; Ruangsupapichat, N.; Parschau, M.; Macia, B.; Katsonis, N.; Harutyunyan, S. R.; Ernst, K.-H.; Feringa, B. L. Electrically Driven Directional Motion of a Four-Wheeled Molecule on a Metal Surface. *Nature* **2011**, *479*, 208–211.
47. Yi, S.; Kaifer, A. E. Determination of the Purity of Cucurbit[*n*]uril (*n* = 7, 8) Host Samples. *J. Org. Chem.* **2011**, *76*, 10275–10278.